Steel and Composite Structures, *Vol. 26, No. 1 (2018) 17-29*
DOI: https://doi.org/10.12989/scs.2018.26.1.017

Postbuckling and nonlinear vibration of composite laminated trapezoidal plates

Guoqing Jiang[1], Fengming Li[*1,2,3] and Chuanzeng Zhang[3]

[1]*College of Mechanical Engineering, Beijing University of Technology, Beijing 100124, China*
[2]*College of Aerospace and Civil Engineering, Harbin Engineering University, Harbin 150001, China*
[3]*Department of Civil Engineering, University of Siegen, D-57068 Siegen, Germany*

(*Received April 6, 2017, Revised September 4, 2017, Accepted September 23, 2017*)

Abstract. The thermal effects on the buckling, postbuckling and nonlinear vibration behaviors of composite laminated trapezoidal plates are studied. Aiming at the complex plate structure and to simulate the temperature distribution of the plate, a finite element method (FEM) is applied in this paper. In the temperature model, based on the thermal diffusion equation, the Galerkin's method is employed to establish the temperature equation of the composite laminated trapezoidal plate. The geometrical nonlinearity of the plate is considered by using the von Karman large deformation theory, and combining the thermal model and aeroelastic model, Hamilton's principle is employed to establish the thermoelastic equation of motion of the composite laminated trapezoidal plate. The thermal buckling and postbuckling of the composite laminated rectangular plate are analyzed to verify the validity and correctness of the present methodology by comparing with the results reported in the literature. Moreover, the effects of the temperature with the ply-angle on the thermal buckling and postbuckling of the composite laminated trapezoidal plates are studied, the thermal effects on the nonlinear vibration behaviors of the composite laminated trapezoidal plates are discussed, and the frequency-response curves are also presented for the different temperatures and ply angles.

Keywords: laminated trapezoidal plates; nonlinear vibration; thermal buckling and postbuckling

1. Introduction

Recently, the composite laminated plates are widely applied in various engineering structures such as aircraft, high-speed trains, automobiles and biological equipments. In reality, the plates are often processed into various shapes according to the practical application requirements, and they are usually used in thermal environments. So it has important practical significance to study the vibration characteristics of the irregular composite laminated plates in the thermal environments. In the previous works, thermal effects on the static and nonlinear dynamic behaviors of plates have been received much attention.

Some researchers have studied the rectangular plates considering the thermal effects. Chen and Chen (1989) applied the finite element method (FEM) to analyze the thermal postbuckling of the laminated composite plates. Bhimaraddi (1993) analyzed the thermal effects on the buckling, postbuckling and nonlinear vibrations of the laminated plates. Liu and Huang (1996) studied the free vibration of the composite laminated plates subjected to temperature changes. Huang and Shen (2004) analyzed the nonlinear vibration and dynamic responses of functionally graded plates in thermal environments. Chen and Lawrence (2006) developed a FEM to investigate the thermal postbuckling of plates. Moradi (2012) and Mansouri used the differential quadrature (DQ) method to investigate the thermal buckling of rectangular composite laminated plates and assumed the composite plate is subjected to a uniform temperature distribution. Chen *et al*. (2013b) used first-order shear deformation plate theory to study the dynamic instability of laminated composite plates under thermal and arbitrary in-plane periodic loads.

Pandey *et al*. (2009) used an analytical approach to analyze the thermoelastic stability of laminated composite plates. Shiau *et al*. (2010) investigated the thermal buckling behavior of composite laminated plates. Zhou *et al*. (2011) performed the three-dimensional analyses for transient coupled thermoelastic responses of a functionally graded rectangular plate. Jeyaray (2013) analyzed the buckling and free vibration behaviors of an isotropic plate under non-uniform thermal load. Chen *et al*. (2013a) considered the temperature-dependent properties to investigate the vibration and stability of the laminated composite plates. Geng *et al*. (2014) developed the experimental and numerical simulation methods to study the dynamic and acoustic responses of a clamped rectangular plate in thermal environments. Pandey and Pradyumna (2015) analyzed the free vibration of the functionally graded sandwich plates in thermal environments using a layer-wise theory. Attia *et al*. (2015) applied the various four variable refined plate theories to analyze the vibration of functionally graded (FG) plates considering the temperature-dependent properties.

Moreover, the irregular plates under thermal environments are also of considerable interest to many

∗Corresponding author, Professor
E-mail: fmli@bjut.edu.cn

ISSN: 1229-9367 (Print), 1598-6233 (Online)

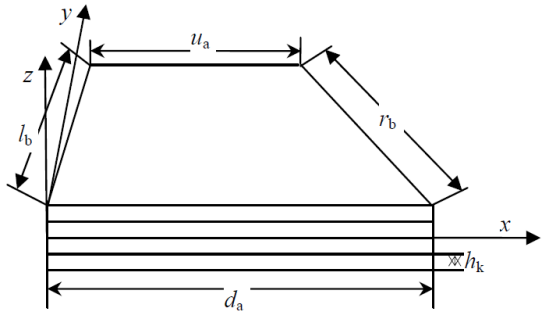

Fig. 1 The composite laminated trapezoidal plate

researchers. Heuer *et al*. (1993) studied the nonlinear random vibrations and thermal buckling of skew plates. Sundararajan *et al*. (2005) investigated the nonlinear free flexural vibrations of the functionally graded rectangular and skew plates in thermal environments. Matsunaga (2005) applied a global higher-order deformation theory to study the thermal buckling of cross-ply laminated composite and sandwich plates. Singha *et al*. (2006) analyzed the thermal effects on the vibration behavior of composite skew plates. Kundu and Sinha (2007) investigated the postbuckling of the laminated composite shells. Malekzadeh *et al*. (2010) studied the three-dimensional free vibration of thick functionally graded annular plates in thermal environments. Vosoughi *et al*. (2011) analyzed the thermal postbuckling of laminated composite skew plates with temperature-dependent properties.

Jaberzadeh *et al*. (2013) used the element-free Galerkin method to analyze the thermal buckling of functionally graded skew and trapezoidal plates with different boundary conditions. Taj *et al*. (2014) investigated the vibration characteristics of the functionally graded skew plate in thermal environments. Gupta and Sharma (2010, 2014) studied the thermal effects on the vibration of the orthotropic trapezoidal plate with linearly varying thickness and the free transverse vibration of the orthotropic thin trapezoidal plate with parabolically varying thickness subjected to a linear temperature distribution.

From the above analyses, it can be observed although there are some previous works devoted to the plate problems with thermal effects, most of them are focused on the rectangular plates, very few works have studied the composite laminated trapezoidal plates, and most of them assumed that the temperature is constant along the thickness of the plate. Moreover, the thermal effects on the nonlinear vibration behaviors have been seldom considered. In our previous works, we have studied the nonlinear vibration characteristics of composite laminated trapezoidal plates (Jiang *et al*. 2016). In this paper, analyses of the thermal effects on the postbuckling and nonlinear vibration behaviors of the composite laminated trapezoidal plates are further conducted. Based on the thermal diffusion equation and the FEM, the heat conduction equation of the composite laminated trapezoidal plate is obtained using the Galerkin method. The geometrical nonlinearity of the plate is considered by means of the von Karman large deflection theory. The thermoelastic equation of motion of the composite laminated trapezoidal plate is established by the FEM and Hamilton's principle. The effects of the ply-angle and the temperature change on the thermal buckling and postbuckling characteristics of the composite laminated trapezoidal plates are studied, the thermal effects on the nonlinear vibration behaviors of the composite laminated trapezoidal plates are discussed, and the frequency-response curves are also presented for the different temperatures and ply-angles.

2. Thermoelastic equation of motion

The composite laminated trapezoidal plate as shown in Fig. 1 is considered. The lengths of the top and bottom edges are u_a and d_a, the lengths of the left and right sides are l_b and r_b, and the thickness of each lamina of the composite laminated plate is h_k.

The displacements of the plate in the *x*-, *y*- and *z*-directions are denoted by *u*, *v* and *w*. And the temperature filed in the trapezoidal plate is in the steady state. In what follows, the variables with the subscripts *x*, *y* and *z* represent the variables in the global coordinate system, and those with the subscripts 1, 2 and 12 represent the variables in the local coordinate system.

2.1 Thermoelastic equation of motion of the composite laminated trapezoidal plate

According to the classical laminate plate theory (CLPT), the displacement components of the composite laminated plate are expressed as

$$u = u_0 - z\frac{\partial w_0}{\partial x}, v = v_0 - z\frac{\partial w_0}{\partial y}, w = w_0, \tag{1}$$

where u_0, v_0 and w_0 denote the in-plane and transverse displacements of the mid-plane in the *x*-, *y*- and *z*-directions, and *z* is the transverse coordinate of the global coordinate system.

According to the von Karman large deformation theory, the nonlinear strain-displacement relations are given by

$$\begin{aligned}\{\varepsilon\} &= \begin{Bmatrix}\varepsilon_x\\ \varepsilon_y\\ \gamma_{xy}\end{Bmatrix} = \{\varepsilon_0\} + \{\varepsilon_l\} + z\{k\}\\ &= \begin{Bmatrix}\dfrac{\partial u_0}{\partial x}\\ \dfrac{\partial v_0}{\partial y}\\ \dfrac{\partial v_0}{\partial x} + \dfrac{\partial u_0}{\partial y}\end{Bmatrix} + \begin{Bmatrix}\dfrac{1}{2}\left(\dfrac{\partial w_0}{\partial x}\right)^2\\ \dfrac{1}{2}\left(\dfrac{\partial w_0}{\partial y}\right)^2\\ \dfrac{\partial w_0}{\partial x}\dfrac{\partial w_0}{\partial y}\end{Bmatrix} + \begin{Bmatrix}-z\dfrac{\partial^2 w_0}{\partial x^2}\\ -z\dfrac{\partial^2 w_0}{\partial y^2}\\ -2z\dfrac{\partial^2 w_0}{\partial x\partial y}\end{Bmatrix}\end{aligned} \tag{2}$$

where $\{\varepsilon_0\}$ and $\{\varepsilon_l\}$ represent the membrane strains, and $\{k\}$ represents the bending curvature.

Considering the problem of plane-stress, the strains induced by the thermal effect are given by

$$\{\varepsilon_t'\} = \begin{Bmatrix}\varepsilon_1'\\ \varepsilon_2'\\ \gamma_{12}'\end{Bmatrix} = \begin{Bmatrix}\alpha_1\Delta T\\ \alpha_2\Delta T\\ 0\end{Bmatrix} = \{\alpha\}\Delta T, \tag{3}$$

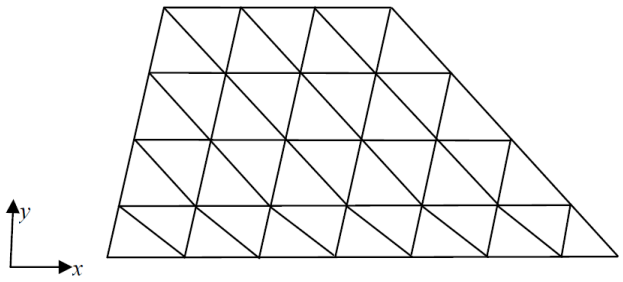

Fig. 2 The form of the mid-plane of the trapezoidal plate divided by displacement elements

where α_1 and α_2 represent the coefficients of the linear expansion, $\Delta T=T_t-T_0$ in which ΔT, T_0 and T_t represent the temperature change, and the initial and the terminal temperatures at an arbitrary point of the plate.

According to the orthotropic property of the composite laminated material and by means of Eq. (3), the constitutive equations of the kth lamina in the global coordinate system are given by

$$\{\sigma\}=\begin{Bmatrix}\sigma_x\\ \sigma_y\\ \tau_{xy}\end{Bmatrix}=[D][Q][D]^T\left(\{\varepsilon\}-\{\alpha\}\Delta T\right) \tag{4}$$
$$=\left[\bar{Q}\right]\left(\{\varepsilon\}-\{\alpha\}\Delta T\right),$$

where $[D]$ is the coordinate transformation matrix, and $[Q]$ is the elasticity matrix.

In order to match the complex boundary shapes of the trapezoidal plate, the triangular plate elements are used to discretize the mid-plane of the trapezoidal plate, and the discrete schematic is shown in Fig. 2.

Thus, the displacements of the element-nodes can be divided into the bending components (w, φ_x, φ_y) and the axial components (u, v). So the displacements at an arbitrary point of the elements can be obtained as follows:

$$w_0=\{H_w\}^T\{w_b\},\quad u_0=\{H_u\}^T\{w_u\},\quad v_0=\{H_v\}^T\{w_v\} \tag{5}$$

where

$$\{w_b\}=\{w_1\quad \phi_{x1}\quad \phi_{y1}\quad w_2\quad \phi_{x2}\quad \phi_{y2}\quad w_3\quad \phi_{x3}\quad \phi_{y3}\}^T,$$
$$\{w_u\}=\{u_1\quad u_2\quad u_3\}^T,\{w_v\}=\{v_1\quad v_2\quad v_3\}^T,$$
$$\{H_w\}=\{N_1\quad N_{x1}\quad N_{y1}\quad N_2\quad N_{x2}\quad N_{y2}\quad N_3\quad N_{x3}\quad N_{y3}\}^T,$$
$$\{H_u\}=\{L_1\quad L_2\quad L_3\}^T,\{H_v\}=\{L_1\quad L_2\quad L_3\}^T,$$
$$N_i=L_i+L_i^2L_j+L_i^2L_m-L_iL_j^2-L_iL_m^2,$$
$$N_{xi}=b_jL_i^2L_m-b_mL_i^2L_j+\left(b_j-b_m\right)L_iL_jL_m/2,$$
$$N_{yi}=c_jL_i^2L_m-c_mL_i^2L_j+\left(c_j-c_m\right)L_iL_jL_m/2,$$
$$a_i=x_jy_m-x_my_j,b_i=y_j-y_m,c_i=x_m-x_j,$$
$$i=1\text{-}2\text{-}3,\ j=2\text{-}3\text{-}1,\ m=3\text{-}1\text{-}2,$$

in which L_1, L_2, L_3 are the area coordinates of the triangular plate elements.

Since Eq. (5) is expressed in the natural coordinate system and all other formulas are in the physical coordinate system, they should be transformed into the natural coordinate system. The transformation relationship is expressed as

$$\begin{Bmatrix}L_1\\ L_2\\ L_3\end{Bmatrix}=\frac{1}{2A}\begin{bmatrix}a_1 & b_1 & c_1\\ a_2 & b_2 & c_2\\ a_3 & b_3 & c_3\end{bmatrix}\begin{Bmatrix}1\\ x\\ y\end{Bmatrix}, \tag{6}$$
$$dxdy=|J|dL_1dL_2=2AdL_1dL_2$$

where J is the Jacobian matrix, and A is the surface area of the plate.

Hamilton's principle is used to formulate the equation of motion of the plate, which can be stated as

$$\int_{t_1}^{t_2}\delta(T-U)dt+\int_{t_1}^{t_2}\delta W dt=0, \tag{7}$$

where T, U and W are the kinetic energy, the strain energy and the work done by the external loads, and they are given by

$$T=\frac{1}{2}\int_V\rho\left(\dot{u}^2+\dot{v}^2+\dot{w}^2\right)dV \tag{8a}$$

$$U=\frac{1}{2}\int_V\{\varepsilon\}^T\{\sigma\}dV \tag{8b}$$

$$W=\sum_{i=1}^{N}\{w_b\}^T\{H_w\}_{(x_i,y_i)}F_i \tag{8c}$$

where V is the volume of the plate, ρ is the mass density of the material, and F_i is the concentrated force at the point (x_i, y_i).

Substituting Eqs. (1)-(5) into Eq. (8) and then into Eq. (7), the thermoelastic equation of motion of the element is obtained. By assembling the element mass and stiffness matrices into the global ones, the thermoelastic equation of motion of the composite laminated trapezoidal plates can be obtained as follows:

$$[M]\{\ddot{W}\}+[C]\{\dot{W}\}+[K_l]\{W\}+[K_{nl}]\{W\}$$
$$-[K_t]\{W\}=\{F_t\}+\{F\}, \tag{9}$$

where $\{w\}=[u_1, v_1, w_1, \varphi_{x1}, \varphi_{y1}\ldots u_n, v_n, w_n, \varphi_{xn}, \varphi_{yn}]^T$ is the nodal displacement vector in which n is the number of the node of the trapezoidal plate, $[M]$ is the mass matrix, $[C]$ is the structural damping matrix, $[K_l]$ and $[K_{nl}]$ are the linear and nonlinear stiffness matrices, $[K_t]$ is the thermal stiffness matrix, $\{F_t\}$ is the temperature-induced force vector, and $\{F\}$ is the external excitation vector. The elements of the matrices and the vectors in Eq. (9) are listed in Appendix A.

2.2 The temperature equation of the trapezoidal plate

We assume that only the top and the bottom surfaces of the trapezoidal plate have heat convection, and after heat exchange, the temperature at an arbitrary point of the plate is constant. In order to facilitate the element assembly, the triple prism element is adopted as the temperature element. Fig. 3 shows the combined form of the temperature element and the displacement element. The indices i, j, k and 1-6 represent the triangular element and the triple prism element, respectively.

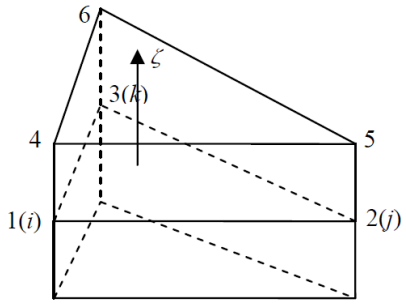

Fig. 3 Combined form of the temperature element and the displacement element in the composite laminated trapezoidal plate

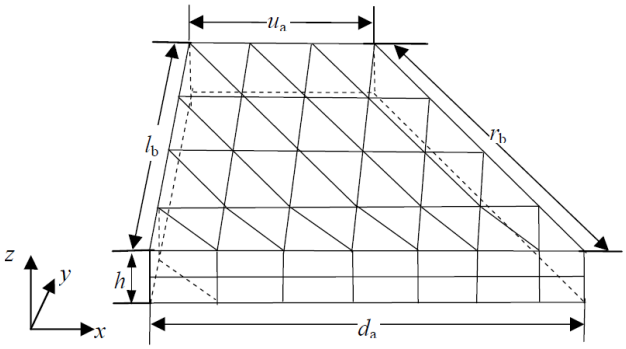

Fig. 4 The form of the trapezoidal plate divided by the temperature elements

In order to facilitate the element assembly for the whole composite laminated trapezoidal plate, the forms of the temperature elements for the trapezoidal plate are divided as those presented in Fig. 4. It is advantageous to divide the meshes in this way for the present analysis.

Next, the triple prism element is applied to discretize the trapezoidal plate. So the temperature at an arbitrary point of the element can be written as follows

$$T_t = \{H_t\}^T \{T_b\}, \tag{10}$$

where

$$\{T_b\} = \{T_1 \quad T_2 \quad T_3 \quad T_4 \quad T_5 \quad T_6\}^T,$$
$$\{H_t\} = \{N_1 \quad N_2 \quad N_3 \quad N_4 \quad N_5 \quad N_6\}^T,$$
$$N_1 = \frac{1}{2}L_1(1+\zeta), N_2 = \frac{1}{2}L_2(1+\zeta),$$
$$N_3 = \frac{1}{2}L_3(1+\zeta), N_4 = \frac{1}{2}L_1(1+\zeta),$$
$$N_5 = \frac{1}{2}L_2(1+\zeta), N_6 = \frac{1}{2}L_3(1+\zeta),$$

in which T_i (i=1-6) are the temperature values at the nodes of the triple prism element.

For the steady state temperature field, the heat conduction equation can be written as follows

$$\lambda_x \frac{\partial^2 T_t}{\partial x^2} + \lambda_y \frac{\partial^2 T_t}{\partial y^2} + \lambda_z \frac{\partial^2 T_t}{\partial z^2} = 0, \tag{11}$$

where λ_x, λ_y, and λ_z represent the thermal conductivity coefficients in the x-, y- and z-directions.

In order to solve Eq. (11), according to the Galerkin method and by means of Eq. (10), the six residual equations can be obtained as follows

$$\iiint_{V^e} \{H_t\}^T \left(\lambda_x \frac{\partial^2 T_b}{\partial x^2} + \lambda_y \frac{\partial^2 T_b}{\partial y^2} + \lambda_z \frac{\partial^2 T_b}{\partial z^2} \right) dV = 0. \tag{12}$$

According to the thermal boundary condition, the following relationship can be obtained

$$\lambda_z \frac{\partial T_t}{\partial z} = -\beta(T_t - T_f), \tag{13}$$

where β is the surface heat-transfer coefficient, and T_f is the temperature of the environment.

By virtue of Eq. (13), the temperature equation of the element can be obtained by solving Eq. (12), and then by assembling the element mass and stiffness matrices of the temperature element into the global ones, the temperature equation of the composite laminated trapezoidal plates can be obtained as

$$[K]\{T_t\} + [K_{tb1}]\{T_t\} + [K_{tb2}]\{T_t\} = \{F_{t1}\}T_{f1} + \{F_{t2}\}T_{f2}, \tag{14}$$

where $\{T_t\}$ is the nodal temperature vector, $[K]$ is the heat transfer matrix, $[K_{tb1}]$ and $[K_{tb2}]$ are the heat transfer matrices which are caused by the convection boundary, $\{F_{t1}\}$ and $\{F_{t2}\}$ are the thermal load vectors, and T_{f1} and T_{f2} are the initial and terminal temperatures of the environment. The elements of the matrices and the vectors in Eq. (14) are listed in Appendix B.

In the same way, these formulas established should be transformed into the natural coordinate system and the transformation relationships are expressed as

$$\begin{bmatrix} L_1 \\ L_2 \\ L_3 \\ \zeta \end{bmatrix} = \begin{bmatrix} \frac{a_1}{2A} & \frac{b_1}{2A} & \frac{c_1}{2A} & 0 \\ \frac{a_2}{2A} & \frac{b_2}{2A} & \frac{c_2}{2A} & 0 \\ \frac{a_3}{2A} & \frac{b_3}{2A} & \frac{c_3}{2A} & 0 \\ 0 & 0 & 0 & \frac{2}{h} \end{bmatrix} \begin{bmatrix} 1 \\ x \\ y \\ z \end{bmatrix} + \begin{bmatrix} 0 \\ 0 \\ 0 \\ \frac{-2z_i}{h} - 1 \end{bmatrix} \tag{15}$$

$$dxdydz = |J| dL_1 dL_2 d\zeta = h dL_1 dL_2 d\zeta, \tag{16}$$

where J is the Jacobian matrix, and A is the surface area of the plate, h is the thickness of the element, and z_i is the height of the bottom surface of the triple prism element.

Through Eq. (14), the temperature distributions in the trapezoidal plate can be obtained. Then by substituting the computed temperature field into Eq. (9), the thermal effects on the postbuckling and nonlinear vibration behaviors of the composite laminated trapezoidal plates can be analyzed. It should be noted here that the thermal force vector in Eq. (9) is related to the boundary conditions. If the boundary of the plate is clamped, it is unnecessary to consider the thermal force vector. But for the simply supported boundary conditions, the temperature induced forces may have great influences on the mechanical properties of the composite laminated trapezoidal plates.

By solving Eq. (9), the nonlinear frequency and nonlinear frequency ratio can be obtained using an iterative solution procedure. The main steps of the procedure are as follows:

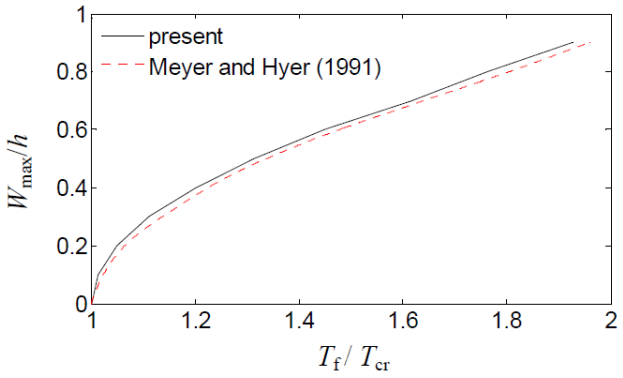

Fig. 5 The thermal postbuckling of the simply supported composite laminated plates

a) Given the initial and terminal temperatures of the environment, the thermal stiffness matrix $[K_t]$ can be known.

b) Then, at the first step of the iteration, the nonlinear stiffness matrix is neglected and the linear eigenvector $\{\delta\}$ is calculated.

c) For specifying a value for the maximum deflection parameter w_{max}/h, the eigenvector $\{\delta\}$ is normalized so that the maximum nodal displacement becomes w_{max}/h.

d) Using the eigenvector $\{\delta\}$ obtained in step (c), the nonlinear stiffness matrix $[K_{nl}]$ is evaluated. At this moment, the nonlinear stiffness is assumed to be known, and also Eq. (9) can be treated linear. Then new eigenvector $\{\delta\}_{NL}$ is obtained.

e) Steps c)-d) are repeated until a convergence of the eigenvalue is achieved. And this eigenvalue is the nonlinear frequency corresponding to the given initial and terminal temperatures of the environment.

f) Steps a)-e) are repeated for the different required maximum deflection parameters w_{max}/h corresponding to the given initial and terminal temperatures of the environment.

g) Steps a)-f) are repeated for the different initial and terminal temperatures.

3. Numerical results and discussions

3.1 Validations of the formulations and the computer codes

In order to verify the validity and the correctness of the equation of motion and the developed MATLAB programs, the thermal buckling results of an isotropic rectangular plate are compared with those of Amabili and Carra (2009) and Liew *et al*. (2003) as shown in Table 1. The material properties and the geometrical parameters of the rectangular plate used in the calculation are: $E_1=E_2=198\times10^9$ Pa, $\mu_{12}=0.3$, $\rho=7850$ kg/m^3, the length and width $a=b=0.1$ m, and the thickness $h=0.001$ m.

The boundary conditions considered here are:

(a) Immovable simply supported condition

$u_0=v_0=w_0=0$, at $x=0$, a and $y=0$, b.

(b) Clamped condition

Table 1 Thermal buckling results of a clamped isotropic rectangular plate.

Number of elements	32	72	162	Amabili and Carra (2009)	Liew (2003)
Buckling temperatures	0.299	0.314	0.326	0.34	0.337

$u_0=v_0=w_0=\varphi_x=\varphi_y=0$, at $x=0$, a and $y=0$, b.

Furthermore, the thermal postbuckling results of the immovable simply supported composite laminated plate are compared with those of Meyers and Hyer (1991) and shown in Fig. 5, in which T_{cr} represents the critical buckling temperature and T_f is the terminal temperature of the environment. The transverse deflection amplitude W_{max} is evaluated for a simply supported composite laminated square plate. The material properties and the geometrical sizes of the eight-layer composite laminated square plate used in the calculation are: $E_1=155\times10^9$ Pa, $E_2=8.07\times10^9$ Pa, $G_{12}=4.55\times10^9$ Pa, $\rho=7850$ kg/m^3, $\mu_{12}=0.22$, the length and width $a=b=0.1524$ m, the single lamina thickness $h=1.27\times10^{-4}$m, and the ply-angle is $[45°/-45°/0°/90°]_s$.

It can be seen from Table 1 and Fig. 5 that the present results match quite well with those of the references, which verifies that the thermoelastic equation of motion obtained in this paper and the developed MATLAB programs are correct.

3.2 Selection of the model parameters

In this paper, the material (graphite/epoxy) properties of the considered composite laminated trapezoidal plate are: $E_1=181\times10^9$ Pa, $E_2=10.3\times10^9$ Pa, $G_{12}=7.17\times10^9$ Pa, $\rho=1389.23$ kg/m^3, and $\mu_{12}=0.28$. The coefficients of the linear thermal expansion are $\alpha_1=0.02\times10^6$/℃ and $\alpha_2=22.5\times10^6$/℃, the thermal conductivity coefficients are $\lambda_x=0.1$W/(m·℃), $\lambda_y=0.15$ W/(m·℃) and $\lambda_z=0.2$ W/(m·℃), and the surface heat-transfer coefficient is $\beta=20$ W/(m^2·℃). Assume that the initial temperature of the environment is 30℃. The geometrical sizes of the trapezoidal plate are: $d_a=0.3$ m, $u_a=0.135$ m, $l_b=0.21$ m, $r_b=0.26$ m, and the thickness of the laminated trapezoidal plate with four laminas is $h=0.0025$ m. The height of the trapezoidal plate is denoted by L. The boundary conditions are as follows:

$u_0=v_0=w_0=\varphi_x=\varphi_y=0$, at $y=0$ and L, and at l_b and r_b edges.

3.3 Thermal buckling and postbuckling analysis

In this section, the thermal buckling and postbuckling of the composite laminated trapezoidal plate are investigated. Table 2 shows the non-dimensional maximum buckling displacements with respect to the terminal temperature values of the environment for the different ply-angles. In the table, the symbol "--" means that the plate has not yet been buckled at this temperature.

According to Table 2, the relationship curves of the maximum buckling displacement and the terminal temperature of the environment of the trapezoidal plate with the different ply-angles are displayed in Fig. 6. In the figure, the point A is the critical buckling temperature. It is

Table 2 The maximum buckling displacement (w_{max}/h) of the composite laminated trapezoidal plates

T_f \ Ply angle	$[0^\circ/0^\circ]_s$	$[10^\circ/-10^\circ]_s$	$[20^\circ/-20^\circ]_s$	$[30^\circ/-30^\circ]_s$	$[45^\circ/-45^\circ]_s$	$[60^\circ/-60^\circ]_s$	$[75^\circ/-75^\circ]_s$	$[90^\circ/-90^\circ]_s$
80	--	--	--	--	--	--	0.3770	0.5276
90	--	--	--	--	--	0.2882	0.6436	0.7528
100	--	--	--	--	--	0.5536	0.8304	0.9192
120	--	--	--	--	0.3123	0.8800	1.1124	1.1760
140	--	--	--	--	0.6536	1.1228	1.3316	1.3808
160	--	--	--	--	0.8792	1.3252	1.5168	1.5572
180	--	--	--	0.1929	1.0628	1.5020	1.6808	1.7136
200	--	--	--	0.4624	1.2220	1.6604	1.8296	1.8560
220	--	--	--	0.6296	1.3644	1.8044	1.9672	1.9868
240	--	--	0.1940	0.7648	1.4944	1.9364	2.0960	2.1084
260	0.1706	0.1279	0.2956	0.8820	1.6144	2.0592	2.2176	2.2228
280	0.2695	0.2456	0.3609	0.9880	1.7268	2.1744	2.3320	2.3300
300	0.3406	0.3231	0.4198	1.0844	1.8324	2.2832	2.4412	2.4412

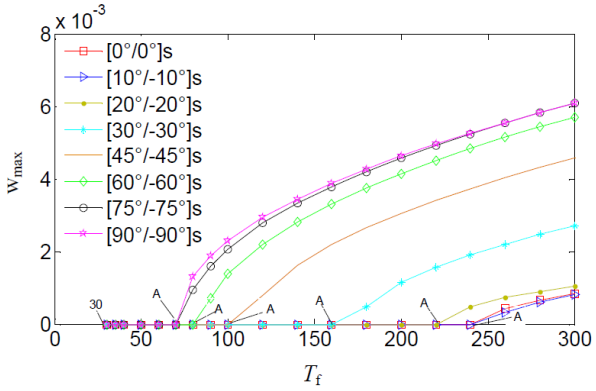

Fig. 6 Thermal postbuckling displacements of the trapezoidal plate under the different ply-angles

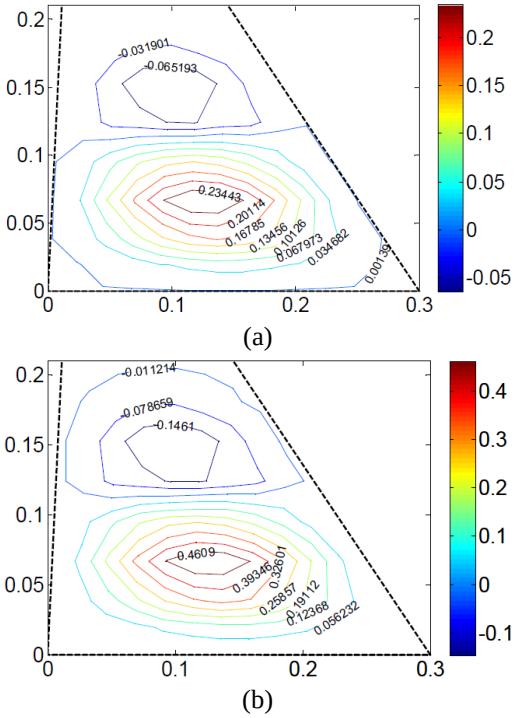

Fig. 7 The contours of the non-dimensional displacement amplitude (w/h) of the trapezoidal plate under the thermal postbuckling at the ply-angle [0°/0°]s for the different temperatures, (a) 260℃, and (b) 300℃

observed from the figure that when the environment temperature exceeds the critical buckling temperature, the plate will have the buckling displacement, which means that the equilibrium position of the plate has been changed to this buckling displacement. For the given ply-angle and with the environmental temperature increasing, the growth rate of the buckling displacement is gradually smaller. And with the ply-angle increasing from $[0^\circ/0^\circ]_s$ to $[90^\circ/-90^\circ]_s$, the critical buckling temperature reduces gradually. The buckling displacement is small for a small ply-angle. Thus, for a small ply-angle the effect of the environmental temperature on the buckling properties of the composite laminated trapezoidal plate is weak.

The contours of the non-dimensional displacement amplitude of the composite laminated trapezoidal plate under the thermal postbuckling at the ply-angles $[0^\circ/0^\circ]_s$ and $[10^\circ/-10^\circ]_s$ for the different temperatures are shown in Figs. 7 and 8. With the temperature increasing, it can be seen from the figures that the areas where the contours appear are smaller and they have a tendency to move to the top edge, and it also can be found that the maximum displacement amplitudes of the plate are higher. This is because that the energy is localized on the point of the maximum displacement amplitude, and the amplitude ratio between the maximum displacement amplitude and that at the edge of the plate increases.

Next, for a fixed temperature, the displacement amplitude of the thermal postbuckling for different ply-angles of the trapezoidal plate is studied. Fig. 9 shows the contours of the non-dimensional displacement amplitude at the temperature 300℃ for the different ply-angles. It can be observed from the figure that with the ply-angle increasing, the maximum displacement amplitude of the plate becomes higher, the position of the maximum displacement amplitude moves towards the top plate edge, the area where the amplitude is relatively large on the plate becomes long and narrow, and the displacement amplitude at the sharp

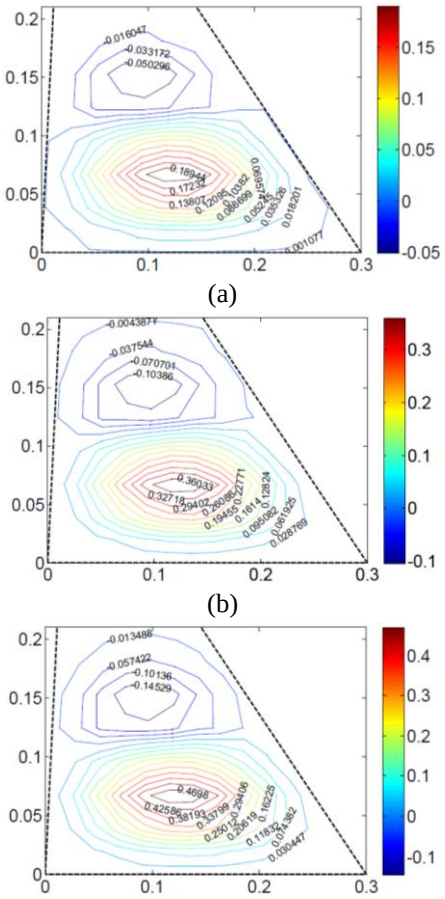

(a) (b) (c)

Fig. 8 The contours of the non-dimensional displacement amplitude (w/h) of the trapezoidal plate under the thermal postbuckling at the ply-angle [10°/-10°]s for the different temperatures, (a) 260℃, (b) 280℃, and (c) 300℃

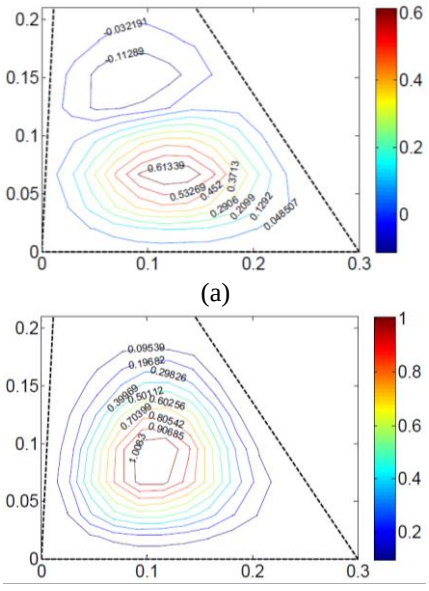

(a) (b)

Fig. 9 The contours of the non-dimensional displacement amplitude (w/h) of the trapezoidal plate under the thermal postbuckling at the temperature 300℃ for the different ply-angles, (a) [20°/-20°]s, (b) [30°/-30°]s, (c) [45°/-45°]s, (d) [60°/-60°]s, (e) [75°/-75°]s, and (f) [90°/-90°]s

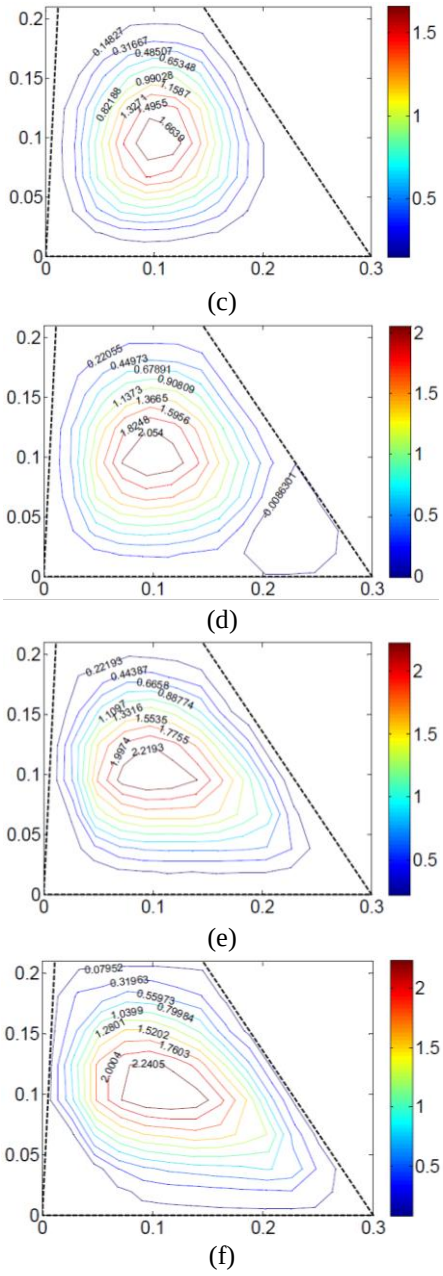

(c) (d) (e) (f)

Fig. 9 Continued

corner is larger. Through the figure it can also be concluded that the contour area where the contour appears decreases with the ply-angle increasing from $[0^\circ/0^\circ]_s$ to $[45^\circ/-45^\circ]_s$, and then it increases with the ply-angle increasing from $[45^\circ/-45^\circ]_s$ to $[90^\circ/-90^\circ]_s$. It means that the energy at the point of the maximum displacement amplitude becomes most focused for the ply-angle $[45^\circ/-45^\circ]_s$. It can be found from Figs. 7-9 that when the ply-angle is lower than $[30^\circ/-30^\circ]_s$, the amplitude distribution has two peaks, the part of the contours near the top plate side is concave, and near the bottom plate side is gibbous, and when the ply-angle is larger than $[30^\circ/-30^\circ]_s$, the amplitude distribution only has one peak.

3.4 Thermal effects on the nonlinear vibration behaviors

Table 3 The natural frequency (ω_L /10^3) of the linear composite laminated trapezoidal plates

Ply angle / T_f	$[0^\circ/0^\circ]_s$	$[10^\circ/-10^\circ]_s$	$[20^\circ/-20^\circ]_s$	$[30^\circ/-30^\circ]_s$	$[45^\circ/-45^\circ]_s$	$[60^\circ/-60^\circ]_s$	$[75^\circ/-75^\circ]_s$	$[90^\circ/-90^\circ]_s$
30(ΔT=0)	3.7365	3.9739	4.2442	4.4589	4.5722	4.4611	4.2843	4.1582
40	3.6779	3.9078	4.1496	4.3106	4.3063	4.0655	3.7949	3.6313
50	3.6170	3.8396	4.0521	4.1562	4.0200	3.6198	3.2218	3.0015
60	3.5534	3.7689	3.9515	3.9951	3.7079	3.1004	2.5040	2.1755
70	3.4869	3.6954	3.8476	3.8263	3.3622	2.4570	1.4269	0.5640
80	3.4171	3.6190	3.7398	3.6486	2.9701	1.5328	--	--
90	3.3435	3.5391	3.6279	3.4605	2.5083	--	--	--
100	3.2655	3.4554	3.5111	3.2603	1.9243	--	--	--
120	3.0940	3.2740	3.2603	2.8117	--	--	--	--
140	2.8963	3.0695	2.9795	2.2652	--	--	--	--
160	2.6634	2.8338	2.6556	1.5136	--	--	--	--
180	2.3820	2.5551	2.2632	--	--	--	--	--
200	2.0302	2.2141	1.7446	--	--	--	--	--
220	1.5612	1.7728	0.8734	--	--	--	--	--
240	0.7927	1.1183	--	--	--	--	--	--

Table 4 The frequency ratios (ω_{NL} /ω_L) of the nonlinear and linear composite laminated trapezoidal plates at the ply-angle $[10^\circ/-10^\circ]_s$ under different environmental temperatures

w_{max}/h / T_f	0.1	0.3	0.5	0.7	0.9	1	1.1	1.2	1.3
30(ΔT=0)	1.00295	1.02622	1.07103	1.13453	1.21335	1.25750	1.30433	1.35353	1.40473
40	1.00307	1.02725	1.07375	1.13951	1.22095	1.26647	1.31469	1.36535	1.41794
50	1.00320	1.02839	1.07677	1.14501	1.22930	1.27634	1.32612	1.37819	1.43233
60	1.00335	1.02967	1.08013	1.15112	1.23851	1.28721	1.33865	1.39238	1.44815
70	1.00351	1.03111	1.08391	1.15792	1.24881	1.29930	1.35248	1.40810	1.46563
80	1.00370	1.03275	1.08818	1.16563	1.26036	1.31281	1.36804	1.42559	1.48504
90	1.00392	1.03463	1.09306	1.17440	1.27344	1.32808	1.38547	1.44520	1.51000
100	1.00417	1.03679	1.09867	1.18440	1.28826	1.34539	1.40523	1.46727	--
120	1.00481	1.04231	1.11285	1.20945	1.32513	1.38808	1.45374	1.52155	--
140	1.00573	1.05023	1.13292	1.24443	1.37578	1.44652	1.51972	--	--
160	1.00716	1.06227	1.16285	1.29560	1.44873	1.53024	--	--	--
180	1.00944	1.08142	1.21019	1.37569	1.56072	1.65743	--	--	--
200	1.01320	1.11361	1.28982	1.50649	1.74392	1.88230	--	--	--
220	1.01956	1.16488	1.41417	1.72678	2.07961	--	--	--	--
240	1.04698	1.36698	1.85235	2.41160	3.01123	--	--	--	--

In this section, the thermal effects on the nonlinear vibration behaviors of the composite laminated trapezoidal plates are investigated. Table 3 shows the natural frequencies corresponding to the linear system with respect to the terminal environmental temperature for the different ply-angles. In the table, ω_L denotes the natural frequency of the linear composite trapezoidal plate, the symbol "--" signifies that the plate has not yet been buckled at this temperature, and the equilibrium position of the vibration is changeable. It can be seen from the table that the natural frequency of the linear composite plate is higher with the ply-angle increasing from $[0^\circ/0^\circ]$ to $[90^\circ/-90^\circ]_s$ for a fixed temperature, and only when the ply-angles are $[0^\circ/0^\circ]_s$ and $[10^\circ/-10^\circ]_s$, the frequency can be obtained at the temperature 240°C. It can be concluded that if the trapezoidal plate is applied in the low temperature environment, the ply-angle of the plate should be designed near to $[90^\circ/-90^\circ]_s$, and if the trapezoidal plate is applied in the high temperature environment, the ply-angle of the plate should be designed near to $[0^\circ/0^\circ]_s$.

Next, considering the nonlinear effects, the frequency ratios (ω_{NL}/ω_L) of the nonlinear and linear composite trapezoidal plates with respect to the terminal temperature of the environment at the ply-angle $[10^\circ/-10^\circ]_s$ for the different maximum displacement amplitudes are shown in Table 4. In the table, ω_{NL} denotes the frequency corresponding to the nonlinear composite trapezoidal plate, and the symbol "--" means that the frequency of the nonlinear system can not be obtained. This is because of the fact that for a fixed temperature, when the maximum displacement amplitude of the trapezoidal plate exceeds a critical value, the vibration behaviors of the plate may be affected by the strong nonlinearity and this can lead to the uncertain vibration behaviors of the plate, which means that the values of the frequency ratios and other parameters relating with the vibration behaviors are randomly

Table 5 The frequency ratios (ω_{NL} /ω_L) of the nonlinear and linear composite laminated trapezoidal plates with the different ply-angles

T_f	Ply angle \ w_{max}/h	0.1	0.3	0.5	0.7	0.9	1.0	1.2
50℃	$[0^\circ/0^\circ]_s$	1.00362	1.03205	1.08636	1.16237	1.25555	1.30724	1.41864
	$[10^\circ/-10^\circ]_s$	1.00320	1.02839	1.07677	1.14501	1.22930	1.27634	1.37819
	$[30^\circ/-30^\circ]_s$	1.00272	1.02417	1.06554	1.12426	1.19736	1.23842	1.32798
	$[45^\circ/-45^\circ]_s$	1.00293	1.02603	1.07044	1.13319	1.21094	1.25445	1.34903
	$[75^\circ/-75^\circ]_s$	1.00502	1.04423	1.11808	1.21973	1.34248	1.41004	--
	$[90^\circ/-90^\circ]_s$	1.00600	1.05271	1.14009	1.25937	--	--	--
70℃	$[0^\circ/0^\circ]_s$	1.00396	1.03500	1.09406	1.17630	1.27649	1.33182	1.45046
	$[10^\circ/-10^\circ]_s$	1.00351	1.03111	1.08391	1.15792	1.24881	1.29930	1.40810
	$[30^\circ/-30^\circ]_s$	1.00324	1.02870	1.07751	1.14620	1.23089	1.27811	1.38041
	$[45^\circ/-45^\circ]_s$	1.00429	1.03782	1.10124	1.18888	1.29497	1.35336	1.47842
	$[75^\circ/-75^\circ]_s$	1.02657	1.21752	1.52600	1.89157	2.28441	2.48675	--
	$[90^\circ/-90^\circ]_s$	1.16506	2.05138	3.14048	4.27274	--	--	--

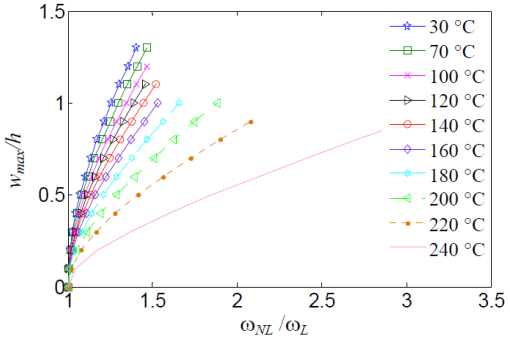

Fig. 10 The relationship curves of the maximum displacement amplitudes and the frequency ratios (ω_{NL}/ω_L) of the nonlinear and linear composite laminated trapezoidal plates at the ply-angle $[10°/-10°]_s$ under the different terminal environmental temperatures

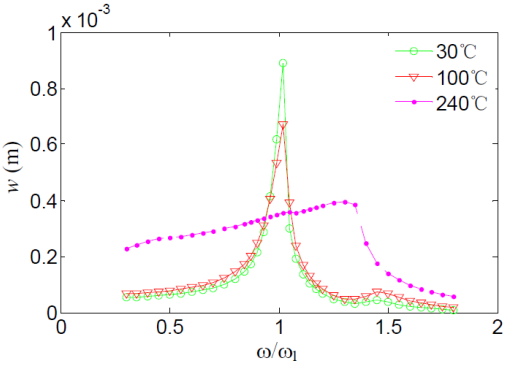

Fig. 11 The frequency-response curves of the laminated trapezoidal plate at the ply-angle $[10°/-10°]_s$ subjected to the external force 19N and different temperatures

changeable with the time. With the temperature increasing, the stiffness of the plate is weakened, and the effect of nonlinearity is enhanced. Thus, it can be seen from the table that the critical value of the maximum displacement amplitude is decreased.

According to Table 4, the relationship curves of the maximum displacement amplitudes and the the frequency ratios (ω_{NL}/ω_L) of the nonlinear system and linear system under the different terminal environmental temperatures are displayed in Fig. 10. It is observed from the figure that with the displacement amplitude increasing, the frequency ratios increase gradually. For a given displacement amplitude, the effect of the nonlinearity on the frequency becomes severe with the environmental temperature increasing.

Next, the effect of the ply-angle on the frequency ratios of the nonlinear and linear systems at a fixed temperature is studied. Table 5 shows the variations of the frequency ratios (ω_{NL}/ω_L) of the nonlinear and linear composite laminated trapezoidal plates with the different ply-angles. It can be observed that for any environmental temperature and for any fixed displacement amplitude, the frequency ratios decreases with the ply-angle increasing from $[0^\circ/0^\circ]_s$ to $[30^\circ/-30^\circ]_s$, and then increases with the ply-angle increasing from $[30^\circ/-30^\circ]_s$ to $[90^\circ/-90^\circ]_s$. Especially, when the ply-angle is $[30^\circ/-30^\circ]_s$, the influence of the nonlinearity becomes weaker.

The thermal effects on the nonlinear forced vibration properties of the composite laminated trapezoidal plates are also studied. The positions of the harmonic force and the observation point of the frequency-response curves on the trapezoidal plate are all at x=0.09513 and y=0.09532. Assuming that the structural damping is c=0.00225. In the following figures, ω_1 denotes the first natural frequency of the linear composite laminated trapezoidal plate.

Fig. 11 shows the frequency-response curves of the composite laminated trapezoidal plates at the ply-angle $[10^\circ/-10^\circ]_s$ subjected to an external force of 19N and different temperatures. It can be seen from the figure that the displacement amplitude of the first nonlinear resonance becomes smaller with the temperature increasing, and the first nonlinear resonance frequency is higher. Especially, it can be observed that the thermal effect on the nonlinear vibration properties becomes more and more severe with the temperature increasing. Next, the frequency-response curves of the trapezoidal plate at the temperature 100℃ and the external force 19N for the different ply-angles are shown in Fig. 12. It can be noted that both the displacement amplitude and the nonlinear resonance frequency increase with the ply-angle increasing. It should be pointed out that

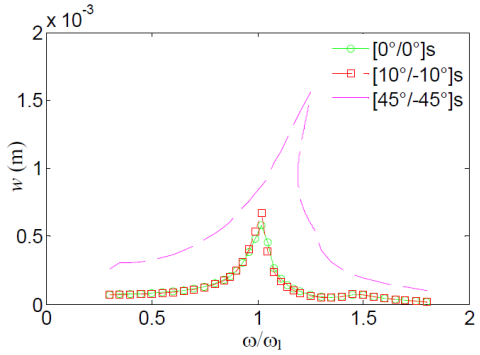

Fig. 12 The frequency-response curves of the trapezoidal plate at the temperature 100℃ and the external force 19N for different ply-angles

the composite laminated trapezoidal plate will be buckled with the ply-angle increasing more than $[45^\circ/-45^\circ]_s$ at the temperature 100℃. This property is presented in Table 3.

Fig. 13 shows the frequency-response curves of the composite laminated trapezoidal plate at the temperature 70℃ and with different ply-angles for different external forces. It can be found that with the external force increasing, for the relatively large ply-angles the frequency-response curves can not be obtained. For example, in Fig. 13(a), the frequency-response curve does not exist for the ply-angle $[90^\circ/-90^\circ]_s$. This phenomenon is due to the properties of the composite laminated trapezoidal plate affected by the strong nonlinearity, which is identical with the results in Table 5.

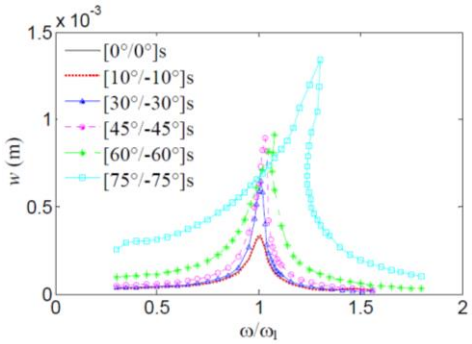

(a) 10 N

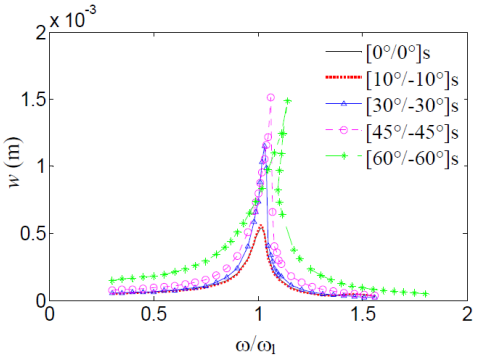

(b) 16 N

Fig. 13 The frequency-response curves of the trapezoidal plate at the temperature 70℃ and with different ply-angles for different external forces. (a) 10 N and (b) 16 N

4. Conclusions

Thermal effects on the buckling, postbuckling and nonlinear vibration behaviors of the composite laminated trapezoidal plates are analyzed. The heat conduction equation of the trapezoidal plate is derived, and the temperature distribution of the plate is obtained. The thermoelastic equation of motion of the composite laminated trapezoidal plate is established by the FEM and Hamilton's principle. The effect of the temperature with the ply-angle on the thermal buckling and postbuckling of the composite laminated trapezoidal plates are studied, and the effects of the temperature on the nonlinear vibration behaviors of the trapezoidal plates are also investigated. From the numerical results, the following conclusions can be drawn:

(1) For the given ply-angle and with the environmental temperature increasing, the growth rate of the maximum displacement amplitudes is gradually smaller. The displacement contour area where the contour of the buckling displacement amplitude appears becomes smaller and it has a tendency to move to the top edge of the trapezoidal plate.

(2) For a fixed temperature and with the ply-angle increasing, the critical buckling temperature reduces gradually. And the buckling displacement is smaller when the ply-angle is close to $[0^\circ/0^\circ]_s$, it means at this ply-angle the thermal effect on the trapezoidal plate is weakest. Moreover, the position of the maximum displacement amplitude moves towards the short side of the trapezoidal plate, and the growth rate of the displacement amplitude at the sharp corner is higher compared with the rest part of the plate. The energy at the point of the maximum displacement amplitude becomes most focused for the ply-angle $[45^\circ/-45^\circ]_s$.

(3) The ply-angle in the range of $[0^\circ/0^\circ]_s$ to $[10^\circ/-10^\circ]_s$ can withstand the highest temperature, and with the environmental temperature increasing the effect of nonlinearity is enhanced. With the ply-angle increasing, the nonlinear frequency may decrease at the beginning and increase later. Especially, when the ply-angle is $[30^\circ/-30^\circ]_s$, the influence of the nonlinearity is very weak.

(4) With the temperature increasing, the displacement amplitude of the first nonlinear resonance becomes smaller and the first nonlinear resonance frequency is higher. Especially, the thermal effect on the nonlinear vibration properties becomes more and more severe with the temperature increasing. With the increase of the ply-angle, both the displacement amplitude and the nonlinear resonance frequency of the composite laminated trapezoidal plates increase.

Acknowledgements

This study was funded by the National Natural Science Foundation of China (grant number 11572007 and

11172084). Fengming Li is grateful to the financial support by the Alexander von Humboldt Foundation for his scientific visit at the Chair of Structural Mechanics, University of Siegen, Germany.

References

Amabili, M. and Carra, S. (2009), "Thermal effects on geometrically nonlinear vibrations of rectangular plates with fixed edges", *J. Sound Vib*., **321**(3-5), 936-954.

Attia, A., Tounsi, A., Adda Bedia, E.A. and Mahmoud, S.R. (2015), "Free vibration analysis of functionally graded plates with temperature-dependent properties using various four variable refined plate theories", *Steel Compos. Struct*., **18**(1), 187-212.

Bhimaraddi, A. (1993), "Nonlinear vibrations of heated antisymmetric angle-ply laminated plates", *Int. J. Solid. Struct*., **30**(9), 1255-1268.

Chen C.S., Tsai T.C., Chen W.R. and Wei C.L. (2013b), "Dynamic stability analysis of laminated composite plates in thermal environments", *Steel Compos. Struct*., **15**(1), 57-79.

Chen, C.S., Chen, C.W., Chen, W.R. and Chang, Y.C. (2013a), "Thermally induced vibration and stability of laminated composite plates with temperature-dependent properties", *Meccanica*, **48**(9), 2311-2323.

Chen, H. and Lawrence, N.V. (2006), "Finite element analysis of post-buckling dynamics in plates. I: An asymptotic approach", *Int. J. Solid. Struct*., **43**(13), 3983-4007.

Chen, L.W. and Chen, L.Y. (1989), "Thermal postbuckling analysis of laminated composite plates by the finite element method", *Compos. Struct*., **12**(4), 257-270.

Geng, Q., Li, H. and Li, Y. (2014), "Dynamic and acoustic response of a clamped rectangular plate in thermal environments: Experiment and numerical simulation", *J. Acoust. Soc. Am*., **135**(5), 2674-2682.

Gupta, A.K. and Sharma, S. (2010), "Thermally induced vibration of orthotropic trapezoidal plate of linearly varying thickness", *J. Vib. Control*, **17**(10), 1591-1598.

Gupta, A.K. and Sharma, S. (2014), "Free transverse vibration of orthotropic thin trapezoidal plate of parabolically varying thickness subjected to linear temperature distribution", *Shock Vib*., **2014**, Article ID 392325.

Heuer, R., Irschik, H. and Ziegler, F. (1993), "Nonlinear random vibrations of thermally buckled skew plates", *Prob. Eng. Mech*., **8**(3-4), 265-271.

Huang, X.L. and Shen, H.S. (2004), "Nonlinear vibration and dynamic response of functionally graded plates in thermal environments", *Int. J. Solid. Struct*., **41**(9-10), 2403-2427.

Jaberzadeh, E., Azhari, M. and Boroomand, B. (2013), "Thermal buckling of functionally graded skew and trapezoidal plates with different boundary conditions using the element-free Galerkin method", *Eur. J. Mech. A/Solid*., **42**, 18-26.

Jeyaray, P. (2013), "Buckling and free vibration behavior of an isotropic plate under nonuniform thermal load", *Int. J. Struct. Stab. Dyn*., **13**(3), 1250071.

Jiang, G.Q., Li, F.M. and Li, X.W. (2016), "Nonlinear vibration analysis of composite laminated trapezoidal plates", *Steel Compos. Struct*., **21**(2), 395-409.

Kundu, C.K. and Sinha, P.K. (2007), "Post buckling analysis of laminated composite shells", *Compos. Struct*., **78**(3), 316-324.

Liew, K.M., Yang J. and Kitipornchai S. (2003), "Postbuckling of piezoelectric FGM plates subject to thermo-electro-mechanical loading", *Int. J. Solid. Struct*., **40**(15), 3869-3892.

Liu, C.F. and Huang, C.H. (1996), "Free vibration of composite laminated plates subjected to temperature changes", *Compos. Struct*., **60**(1), 95-101.

Malekzadeh, P., Shahpari, S.A. and Ziaee, H.R. (2010), "Three-dimensional free vibration of thick functionally graded annular plates in thermal environment", *J. Sound Vib*., **329**(4), 425-442.

Matsunaga, H. (2005), "Thermal buckling of cross-ply laminated composite and sandwich plates according to a global higher-order deformation theory", *Compos. Struct*., **68**(4), 439-454.

Meyers, C.A. and Hyer, M.W. (1991), "Thermal buckling and postbuckling of symmetrically laminated composite plates", *J. Therm. Stress*., **14**(4), 519-540.

Moradi, S. and Mansouri, M.H. (2012), "Thermal buckling analysis of shear deformable laminated orthotropic plates by differential quadrature", *Steel Compos. Struct*., **12**(2), 129-147.

Pandey, R., Shukla, K.K. and Jain, A. (2009), "Thermoelastic stability analysis of laminated composite plates: An analytical approach", *Commun. Nonlin. Sci. Numer. Simul*., **14**(4), 1679-1699.

Pandey, S. and Pradyumna, S. (2015), "Free vibration of functionally graded sandwich plates in thermal environment using a layerwise theory", *Eur. J. Mech. A/Solid*., **51**, 55-66.

Shiau, L.C., Kuo, S.Y. and Chen, C.Y. (2010), "Thermal buckling behavior of composite laminated plates", *Compos. Struct*., **92**(2), 508-514.

Singha, M.K., Ramachandra, L.S. and Bandyopadhyay J.N. (2006), "Vibration behavior of thermally stressed composite skew plate", *J. Sound Vib*., **296**(4-5), 1093-1102.

Sundararajan, N., Prakash, T. and Ganapathi, M. (2005), "Nonlinear free flexural vibrations of functionally graded rectangular and skew plates under thermal environments", *Finite Elem. Anal. Des*., **42**(2), 152-168.

Taj, M.G., Chakrabarti, A. and Prakash, V. (2014), "Vibration characteristics of functionally graded material skew plate in thermal environment", *Int. J. Mech. Aerosp. Indus. Mech. Eng*., **8**(1), 142-153.

Vosoughi, A.R., Malekzadeh, P. and Banan, M.R. (2011), "Thermal postbuckling of laminated composite skew plates with temperature-dependent properties", *Thin Wall. Struct*., **49**(7), 913-922.

Zhou, F.X., Li, S.R. and Lai, Y.M. (2011), "Three-dimensional analysis for transient coupled thermoelastic response of a functionally graded rectangular plate", *J. Sound Vib*., **330**(16), 3990-4001.

CC

Appendix A

The mass matrix, the stiffness matrices and the temperature induced force vector in Eq. (9) are assembled by the corresponding element matrices and element vectors. The mass matrix, the stiffness matrices and the temperature induced force vector for an element are presented in the following.

The mass matrix of the element is given by

$$\left[M^e\right]=\begin{bmatrix} M_{uu} & 0 & M_{ubx} \\ 0 & M_{vv} & M_{vby} \\ M_{bxu} & M_{byv} & M_{bxbx}+M_{byby}+M_{bb} \end{bmatrix},$$

where

$$\left[M_{uu}\right]=\int_v \rho\left[H_u\right]\left[H_u\right]^T dv,$$

$$\left[M_{ubx}\right]=-\int_v \rho\left[H_u\right] z\frac{\partial\left[H_w\right]^T}{\partial x}dv,$$

$$\left[M_{bxu}\right]=-\int_v \rho z\frac{\partial\left[H_w\right]}{\partial x}\left[H_u\right]^T dv,$$

$$\left[M_{bxbx}\right]=\int_v \rho z^2\frac{\partial\left[H_w\right]}{\partial x}\frac{\partial\left[H_w\right]^T}{\partial x}dv,$$

$$\left[M_{vv}\right]=\int_v \rho\left[H_v\right]\left[H_v\right]^T dv,$$

$$\left[M_{vby}\right]=-\int_v \rho\left[H_v\right] z\frac{\partial\left[H_w\right]^T}{\partial y}dv,$$

$$\left[M_{byv}\right]=-\int_v \rho z\frac{\partial\left[H_w\right]}{\partial y}\left[H_v\right]^T dv,$$

$$\left[M_{byby}\right]=\int_v \rho z^2\frac{\partial\left[H_w\right]}{\partial y}\frac{\partial\left[H_w\right]^T}{\partial y}dv,$$

$$\left[M_{bb}\right]=\int_v \rho\left[H_w\right]\left[H_w\right]^T dv.$$

The linear stiffness matrix of the element can be written as

$$\left[K_l^e\right]=\begin{bmatrix} K_{00} & K_{0b} \\ K_{b0} & K_{bb} \end{bmatrix},$$

where

$$\left[K_{00}\right]=\int_A\left[D_0\right]^T\left[A\right]\left[D_0\right]dA,$$

$$\left[K_{0b}\right]=\int_A\left[D_0\right]^T\left[B\right]\left[D_b\right]dA,$$

$$\left[K_{b0}\right]=\int_A\left[D_b\right]^T\left[B\right]\left[D_0\right]dA,$$

$$\left[K_{bb}\right]=\int_A\left[D_b\right]^T\left[C\right]\left[D_b\right]dA,$$

in which

$$\left[D_0\right]=\begin{bmatrix} \dfrac{\partial H_u^T}{\partial x} & 0 \\ 0 & \dfrac{\partial H_v^T}{\partial y} \\ \dfrac{\partial H_u^T}{\partial y} & \dfrac{\partial H_v^T}{\partial x} \end{bmatrix},$$

$$\left[D_b\right]=\begin{bmatrix} -\dfrac{\partial^2 H_w^T}{\partial x^2} \\ -\dfrac{\partial^2 H_w^T}{\partial y^2} \\ -2\dfrac{\partial^2 H_w^T}{\partial x\partial y} \end{bmatrix},$$

$$\left\{\left[A\right],\left[B\right],\left[C\right]\right\}=\sum_{k=1}^{n}\int_{z_{k-1}}^{z_k}\left[\overline{Q}\right]\left\{1 \quad z \quad z^2\right\}dz,$$

where z_k and z_{k-1} are the coordinates of the upper and lower surfaces of the kth lamina in the z-direction.

The nonlinear stiffness matrix of the element is given by

$$\left[K_{nl}^e\right]=\begin{bmatrix} 0 & K_{0l} \\ K_{l0} & K_{ll} \end{bmatrix},$$

where

$$\left[K_{0l}\right]=\frac{1}{2}\int_A\left[D_0\right]^T\left[A\right]\left[D_{l1}\right]\left[D_{l2}\right]dA,$$

$$\left[K_{l0}\right]=\int_A\left[D_{l2}\right]^T\left[D_{l1}\right]^T\left[A\right]\left[D_0\right]dA,$$

$$\left[K_{ll}\right]=\int_A\begin{pmatrix} \frac{1}{2}\left[D_b\right]^T\left[B\right]\left[D_{l1}\right]\left[D_{l2}\right]+ \\ \left[D_{l2}\right]^T\left[D_{l1}\right]^T\left[B\right]\left[D_b\right]+ \\ \frac{1}{2}\left[D_{l2}\right]^T\left[D_{l1}\right]^T\left[A\right]\left[D_{l1}\right]\left[D_{l2}\right] \end{pmatrix}dA,$$

in which

$$\left[D_{l1}\right]=\begin{bmatrix} \dfrac{\partial H_w^T}{\partial x}\left[w_b\right] & 0 \\ 0 & \dfrac{\partial H_w^T}{\partial y}\left[w_b\right] \\ \dfrac{\partial H_w^T}{\partial y}\left[w_b\right] & \dfrac{\partial H_w^T}{\partial x}\left[w_b\right] \end{bmatrix},$$

$$\left[D_{l2}\right]=\begin{bmatrix} \dfrac{\partial H_w^T}{\partial x} \\ \dfrac{\partial H_w^T}{\partial y} \end{bmatrix}.$$

The thermal stiffness matrix of the element can be expressed as

$$\left[K_t^e\right]=\begin{bmatrix} 0 & 0 \\ 0 & \left[K_{bt}\right]-\left[K_{bt0}\right] \end{bmatrix},$$

where

$$\left[K_{bt}\right]=\int_v\left[D_{l2}\right]^T\left[\overline{Q}'_{T11}\right]\left[D_{l2}\right]\left\{H_t\right\}^T\left\{T_b\right\}dv,$$

$$\left[K_{bt0}\right]=\int_v\left[D_{l2}\right]^T\left[\overline{Q}'_{T11}\right]\left[D_{l2}\right]\left\{T_0\right\}dv,$$

in which

$$\left[\overline{Q}'_{T11}\right]=\begin{bmatrix} \overline{Q}_{T11} & \overline{Q}_{T31} \\ \overline{Q}_{T31} & \overline{Q}_{T21} \end{bmatrix},$$

where $\overline{Q}_{T11}$, $\overline{Q}_{T21}$ and $\overline{Q}_{T31}$ are the row vectors of the elasticity matrix $[\overline{Q}]$ of the composite laminated plate in the global coordinate system as can be seen in Eq. (4). The

elasticity matrix $[\bar{Q}]$ is given by

$$\left[\bar{Q}\right]=\begin{bmatrix}\bar{Q}_{T11}\\ \bar{Q}_{T21}\\ \bar{Q}_{T31}\end{bmatrix}_{3*3}.$$

The temperature induced force vector of the element is given by

$$\left\{F_t^e\right\}=\begin{bmatrix}F_{0t}\\ F_{bt}\end{bmatrix}\{T_b\}-\begin{Bmatrix}F_{0t0}\\ F_{bt0}\end{Bmatrix}T_0,$$

where

$$\left[F_{0t}\right]=\int_v\left[D_0\right]^T\left[\bar{Q}_T\right]\{H_t\}^T\,dv,$$

$$\left[F_{0t0}\right]=\int_v\left[D_0\right]^T\left[\bar{Q}_T\right]dv,$$

$$\left[F_{bt}\right]=\int_v z\left[D_b\right]^T\left[\bar{Q}_T\right]\{H_t\}^T\,dv,$$

$$\left[F_{bt0}\right]=\int_v z\left[D_b\right]^T\left[\bar{Q}_T\right]dv.$$

Appendix B

The heat-transfer matrices and the thermal load vectors in Eq. (14) are assembled by the corresponding element matrices and element vectors. The heat-transfer matrices and the thermal load vectors of the element are presented below.

The heat-transfer matrices of the element can be written as

$$\left[K^e\right]=\left[K_{tx}\right]+\left[K_{ty}\right]+\left[K_{tz}\right],$$

$$\left[K_{tb1}^e\right]=\iint_{\Sigma_{123}}\beta\{H_t\}\left[H_t\right]^T\,dxdy,$$

$$\left[K_{tb2}^e\right]=\iint_{\Sigma_{456}}\beta\{H_t\}\left[H_t\right]^T\,dxdy,$$

$$\left[K_{tx}\right]=\iiint_{V^e}\lambda_x\frac{\partial\{H_t\}}{\partial x}\frac{\partial}{\partial x}\left(\left[H_t\right]^T\right)dV,$$

$$\left[K_{ty}\right]=\iiint_{V^e}\lambda_y\frac{\partial\{H_t\}}{\partial y}\frac{\partial}{\partial y}\left(\left[H_t\right]^T\right)dV,$$

$$\left[K_{tz}\right]=\iiint_{V^e}\lambda_z\frac{\partial\{H_t\}}{\partial z}\frac{\partial}{\partial z}\left(\left[H_t\right]^T\right),$$

where Σ_{123} and Σ_{456} represent the areas of the upper and the lower surfaces of the triple prism element.

The thermal load vectors of the element are given by

$$\left\{F_{t1}^e\right\}=\iint_{\Sigma_{123}}\beta\{H_t\}\,dxdy,$$

$$\left\{F_{t2}^e\right\}=\iint_{\Sigma_{456}}\beta\{H_t\}\,dxdy.$$